

Water sorption isotherms and air-drying kinetics modelling of Andean tubers and tuberous roots

Liliana Acurio ^{1,2*}, Ariel Baquerizo ¹, Alexandra Borja ¹, Marcelo Vayas ¹, Purificación García-Segovia ², Javier Martínez-Monzó ² and Marta Igual ^{2*}

¹ Department of Science and Engineering in Food and Biotechnology, Technical University of Ambato. Av. Los Chasquis & Río Payamino, Ambato 180150, Ecuador; lp.acurio@uta.edu.ec (L.A.)

² i-Food Group, Instituto Universitario de Ingeniería de Alimentos-FoodUPV, Universitat Politècnica de València, Camino de Vera s/n, 46021 Valencia, Spain; pugarse@tal.upv.es (P.G.-S.)

* Correspondence: lp.acurio@uta.edu.ec (L.A.); marigra@upvnet.upv.es (M.I.);
Tel.: +593986090742 (L.A.); +34625430677 (M.I.)

Abstract: In recent years, scientific research has focused on studying Andean roots and tubers due to their attractive agricultural and nutritional qualities; however, as they contain high moisture, it is imperative to dry them to extend their useful life. Likewise, analysing food drying kinetics and food stability (regarding water activity) is essential to control moisture removal and marketing progress. The drying process carried out in this study (65°C for 8 hours) showed three clear stages: adaptation, the drying period at a constant velocity, and a third stage with a gradual drop in the drying rate. The experimental data were satisfactorily adjusted to seven mathematical models, highlighting the Page model since it presented higher coefficient of determination values. Likewise, this model estimated mean error and percentage of relative mean deviation values were less than 1. The isotherms showed a type II sigmoidal shape, representing the samples are hygroscopic due to the structural changes suffered by the matrix during the process. Finally, the GAB model showed a higher coefficient of determination. All the Andean tubers and tuberous root flours must be dried until reaching a humidity below 10 g_{water}/g_{dry mass} and stored in environments with a relative humidity lower than 60% to remain stable for longer.

Keywords: ipomoea batatas; tropaeolum tuberosum; arracacia xanthorrhiza, oxalis tuberosa

Citation: To be added by editorial staff during production.

Academic Editor: Firstname Last-name

Published: date



Copyright: © 2023 by the authors. Submitted for possible open access publication under the terms and conditions of the Creative Commons Attribution (CC BY) license (<https://creativecommons.org/licenses/by/4.0/>).

1. Introduction

In recent years, scientific research has focused on studying underutilized autochthonous crops worldwide. Within these crops are the roots produced in the Andes Mountain range. Numerous scientific articles report its peculiar cultivation properties, such as its high adaptability to temperature fluctuation and resistance to pests [1]. There is also scientific evidence of the excellent nutritional qualities of these roots. For example, sweet potato (*Ipomoea batatas* (L.) Lam.) shows high values of protein, fibers, vitamin B, iron, calcium, and bioactive compounds [2]. Mashua (*Tropaeolum tuberosum* Ruiz and Pavón) contains many glucosinolates, polyphenols, isothiocyanates, and anthocyanins that act against plagues and diseases. Also, this root is an excellent provider of vitamin C and provitamin A [3]. Zanahoria blanca (*Arracacia xanthorrhiza* Bancr.) has important values of thiamine, niacin, vitamin A and ascorbic acid [4]. Finally, oca (*Oxalis tuberosa* Molina) presents a high starch quantity (60% of the dry weight) [5], and it is a convenient provider of protein, fructooligosaccharides, iron, and riboflavin [6].

Convection hot air-drying is used mainly in industries to produce dried fruits and vegetables, even though it is not energy efficient and requires more time to reach low moisture. The drying kinetics is essential to control the moisture removal progress and drying variables (drying rate, moisture diffusivity, and activation energy) [7]. The advantage is that this experiment can be conducted on a laboratory scale. Likewise, the drying kinetics modelling is necessary to optimize the process and propose improvements to

the drier before building it on a pilot scale. Food stability is essential in packaging, and a_w is directly related to chemical and microbial changes. Some studies have demonstrated that an a_w increase beyond 0.4 will induce a 50 - 100% increase in the degradation rate [8]. In this sense, the water sorption isotherms can predict the product's shelf life by modelling the possible moisture changes during storage.

The aims of the present work are (1) to determine the corresponding drying kinetics modelling and (2) to determine the water sorption isotherms modelling of sweet potato, mashua, zanahoria blanca, and three varieties of oca (white, yellow, and red).

2. Materials and Methods

2.1. Raw Materials and sample preparation

Sweet potato (*I. batatas* (L.) Lam.), mashua (*T. tuberosum* Ruiz & Pavón), zanahoria blanca (*Arracacia xanthorrhiza* Bancr.), and three varieties of Oca (*O. tuberosa* Molina) white, yellow, and red were purchased from a local market in Ambato, Ecuador. The roots were peeled and cut into slices (2 mm). Slices were pretreated in microwaves (750 W/20 s) and then submerged in water at 4 °C/20 s [9]. This pretreatment was considered necessary because preliminary tests showed that these roots tend to brown due to enzymes and generate undesirable colors. The microwave energy ranges between 1.24×10^{-6} and 1.24×10^{-3} eV, and some studies have demonstrated that it does not affect molecular structure since it is lower than the ionization energies of biological compounds (13.6 eV), bond energies (2–5 eV) and van der Waals interactions (<2 eV) [10,11]. Also, Shen et al. [12] demonstrated a decrease in the double helix structure of potato starch after microwaving at 1000 W, and Lewandowicz et al. [13] showed crystallinity pattern changes after microwaving at 800 W. For this reason, pretreatment was carried out at a lower energy (750 W).

2.2. Determination of drying kinetics

Fresh peeled slices (2 mm) were used to determine the initial water content (x_w). This determination was carried out in a Vaciotem vacuum oven (J.P. Selecta, Barcelona, Spain) set to 103 °C for 48 h. The slices were dried by convection in an air drier (model CD 160, Gander Mountain, Saint Paul, MN, USA) at 65 °C for 8 h, maintaining the air velocity (2 m s⁻¹) constant [14]. The drying temperature was established based on preliminary tests and the results obtained in a study on similar roots grown in the same area (lower temperature for a long time / 60 °C for 24 h) [15].

Samples were placed on a metallic mesh (450×450 mm), allowing a transversal airflow. Drying kinetics were determined by weighing in a precision analytical balance (Mettler Toledo, Greifensee, Switzerland). The weight was measured every 10 min during the first 2 hours and subsequently every 30 min until the drying time was complete (8 h). These experiments were performed on 9 slices of each sample. The water content (x_w) was obtained by vacuum drying the pieces in a vacuum oven (Vaciotem, J.P. Selecta, Barcelona, Spain) at 103 °C for 48 h.

2.2.1. Drying kinetic. Mathematical modelling

Experimental data of drying kinetics were fitted to the models shown in Table 1.

Table 1. Equations used for modelling the drying kinetic.

Model	Equation	Eq. number	References
Newton	$MR = Exp(-kt)$	1	[16]
Page	$MR = Exp(-kt^n)$	2	[17]
Modified Page	$MR = Exp(-kt)^n$	3	[18]
Henderson y Pabis	$MR = a \times Exp(-kt)$	4	[19]
Logarithmic	$MR = a \times Exp(-kt) + c$	5	[20]
Thomson	$MR = 1 + at + bt^2$	6	[21]
Fick	$MR = \frac{X - X_e}{X_o - X_e} = \frac{8}{\pi^2} \sum_{n=1}^{\infty} \frac{1}{(2n-1)^2} \exp\left(-\frac{(2n-1)^2 \pi^2 D_{eff}}{4 \times L^2} \times t\right)$	7	[22]

where MR represents the amount of moisture remaining in the samples reported to the initial moisture content; t is the time (h); n is the drying exponent; a, b, c, and k are the drying constants.

2.3. Determination of water sorption isotherms

The gravimetric method used saturated salt solutions to determine the equilibrium moisture content (Table 2) [23]. The saline solutions used were of reagent grade, and the preparation method was adopted by W Spiess and Wolf [24]. To inhibit microbial growth, thymol was added in $a_w \geq 0.5$. Water sorption experiments were carried out at 20°C (± 1 °C). The sorption isotherm is of particular importance in the determination of a drying end-point, microbiological safety, and predicting shelf life; for this reason, it was chosen to experiment with the average annual temperature (20 \pm 1 °C) [25] reported by the Andean area interested in the development of the technology and where the flour obtained will be marketed (Ambato, Ecuador).

Samples were weighed at regular intervals until constant weight (± 0.0005 g) in a precision analytical balance (Mettler Toledo, Greifensee, Switzerland), the moment in which it is considered the moisture content of samples achieved the equilibrium (12 weeks).

Table 2. Saturated salt solutions are used in the determination of water sorption isotherms.

Name	Nomenclature	a_w^*	Name	Nomenclature	a_w^*
Lithium chloride	LiCl	0.1178	Sodium bromide	NaBr	0.5732
Potassium acetate	CH ₃ CO ₂ K	0.2982	Ammonium sulphate	(NH ₄) ₂ SO ₄	0.8012
Magnesium chloride	MgCl ₂	0.3425			

*Values were determined using the AquaLab 4TE water activity meter (Decagon Devices, Inc., Pullman, WA, USA).

2.3.1. Water sorption isotherms. Mathematical modelling

Experimental data were fitted to the models shown in Table 3.

Table 3. Equations used for modelling the sorption isotherms.

Model	Equation	Equation number	References
Brunauer, Emmett, and Teller (BET)	$X_e = \frac{X_0 \times C \times a_w}{(1 - a_w) \times (1 + (C - 1) \times a_w)}$	8	[26]
Guggenheim, Anderson, and de Boer (GAB)	$X_e = \frac{X_0 \times C \times K \times a_w}{(1 - (K \times a_w)) \times (1 + (C - 1) \times (K \times a_w))}$	9	[27]

where X_e is the equilibrium moisture content ($g_{water}/g_{dry\ mass}$), X_0 is the monolayer moisture content ($g_{water}/g_{dry\ mass}$), C is the empirical constant (dimensionless) for BET and GAB equation; and K is the second empirical constant (dimensionless) for GAB equation.

2.4. Statistical Analysis

The goodness of the fitting was evaluated based on the coefficient of determination (r^2), root mean square error (RMSE), and mean relative percentage deviation (MRPD). Statgraphics Centurion XVII Software, version 17.2.04 (Statgraphics Technologies, Inc., The Plains, VA, USA) was used in the analyses.

3. Results and Discussion

3.1. Drying kinetics

Figure 1a shows the experimental drying kinetic curves. A sudden decrease in humidity is evident in the first 4 h of drying. A trend change is observed since the food has transferred the most significant amount of free water. Figure 1b represents the drying rate curve. An adaptation period is observed in all samples in the first 30 min in which the interface temperature increased to the drying conditions. Subsequently, the constant velocity period was marked for 30 min. In this phase, the samples lose moisture at 1054 \pm 249 $g_{water}/h \times m^2$ until reaching the critical humidity. This phase depends directly on the product, temperature, relative humidity of the air, flow direction, and food thickness [28]. The third stage showed a gradual drop in the drying rate because the superficial layer of water in the food had evaporated entirely. In this period, the drying rate completely decays (18 \pm 9 $g_{water}/h \times m^2$).

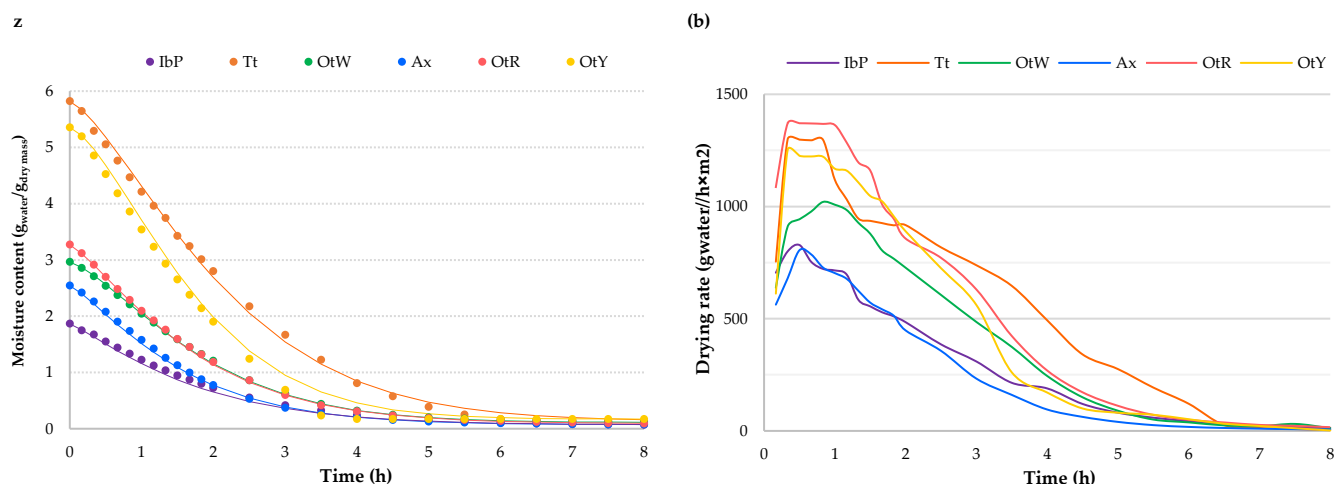


Figure 1. (a) Experimental and estimated drying kinetic curves using Page model, (b) drying rates versus free moisture content ($g_{water}/g_{dry\ mass}$) (IbP: purple sweet potato, Tt: mashua, Ax: zanahoria blanca, OtW: Oca white variety, OtY: Oca yellow variety, OtR: Oca red variety).

3.1.1. Drying kinetics. Mathematical modelling

The coefficient of determination values (r^2) were higher in the Page model (Table 4). Likewise, the RMSE and MRPD were less than 1 in this model. The parameter k represents the movement of moisture inside the food and the transfer to the surface of the air; therefore, higher values represent a faster drying process [29]. The Fick model yielded effective diffusivity values of 2.22 to $2.92 \times 10^{-7} \text{ m}^2/\text{s}$; this value in food oscillates of 1×10^{-6} and $1 \times 10^{-11} \text{ m}^2/\text{s}$ [30]. The variation of the diffusivity depends on the drying conditions (temperature, pressure, and velocity) and the matrix (structure, size, and composition) [31].

Table 4. Parameters obtained in the drying kinetics mathematical modelling.

Sample		Models						
		Newton	Page	Modified Page	Henderson y Pabis	Logarithmic	Thomson	Fick
IbP (Sweet potato)	Model constants	k: 0.691	k: 0.4985 n: 1.173	k: 0.5524 n: 1.173	k: 0.704 a: 1.4597	k: 0.518 a: 1.082 c: 0.0394	a: 0.3497 b: 0.0298	Deff: 2.619×10^{-7}
	Adj. r^2	0.982	0.9923	0.9923	0.988	0.9586	0.99	0.9611
	RMSE	0.134	0.027	4.051	5.0432	0.9293	0.1169	2.232
	MRPD	0.528	0.0265	11.9376	18.6275	4.2325	3.94	10.877
Tt (Mashua)	Model constants	k: 0.66	k: 0.308 n: 1.375	k: 0.4245 n: 1.375	k: 0.738 a: 2.059	k: 0.3136 a: 1.192 c: 0.1465	a: 0.2788 b: 0.0185	Deff: 2.4953×10^{-7}
	Adj. r^2	0.8962	0.989	0.989	0.9244	0.9363	0.9977	0.8627
	RMSE	1.014	0.196	5.582	23.8585	3.5523	23.8585	4.1564
	MRPD	1.086	0.1234	0.1184	22.1583	4.0482	22.1583	5.574
Ax (Zanahoria blanca)	Model constants	k: 0.7684	k: 0.5399 n: 1.2194	k: 0.6164 n: 1.2194	k: 0.75 a: 1.3872	k: 0.6151 a: 1.08 c: 0.0262	a: 0.3746 b: 0.0337	Deff: 2.9196×10^{-7}
	Adj. r^2	0.995	0.9977	0.999	0.9864	0.9636	0.9636	0.996
	RMSE	0.171	0.039	4.4474	6.4694	1.1864	1.1864	2.632
	MRPD	0.521	0.121	9.8944	18.841	4.1582	4.1582	10.49
OtW (Oca white variety)	Model constants	k: 0.7261	k: 0.3893 n: 1.3656	k: 0.2037 n: 1.3656	k: 0.745 a: 1.6428	k: 0.4682 a: 1.14 c: 0.0645	a: 0.3569 b: 0.0296	Deff: 2.762×10^{-7}
	Adj. r^2	0.9845	0.9986	0.999	0.9497	0.952	0.9955	0.9887
	RMSE	1.2457	0.023	4.755	8.122	1.3943	0.16	2.6244
	MRPD	0.9342	0.013	7.5582	19.32	4.11	3.95	8.8533
OtY (Oca yellow variety)	Model constants	k: 0.8689	k: 0.3816 n: 1.46	k: 1.5997 n: 1.291	k: 0.922 a: 2.139	k: 0.444 a: 1.158 c: 0.082	a: 0.3523 b: 0.0285	Deff: 2.7851×10^{-7}
	Adj. r^2	0.9727	0.9921	0.976	0.888	0.9464	0.9953	0.9727
	RMSE	3.129	20.376	5.216	23.1519	1.286	11.6696	4.0237
	MRPD	1.2	18.901	2.684	30.15	4.222	16.451	5.7033
OtR (Oca red variety)	Model constants	k: 0.7743	k: 0.4692 n: 1.243	k: 1.838 n: 1.243	k: 0.7 a: 1.4396	k: 0.527 a: 1.089 c: 0.038	a: 0.3525 b: 0.03	Deff: 2.2283×10^{-7}
	Adj. r^2	0.991	0.998	0.9997	0.9822	0.9685	0.9893	0.9905
	RMSE	0.127	7.4486	4.765	3.78	0.5553	3.151	1.9936
	MRPD	0.226	17.252	11.927	12.376	0.4327	10.973	6.5661

3.2. Water sorption isotherms

The samples showed type II isotherms (Figure 2), also called sigmoidal, since it present an inflection point. Similar results were reported in cassava flour [32]. The isotherm curve showed that the matrix is highly hygroscopic since the higher the environment's relative humidity, the greater the flour's capacity for the water molecules' adsorption. This

shows that the drying and grinding process causes structural changes in the food matrix that influence an increase in the active points of water adsorption [33].

3.2.1. Water sorption isotherms. Mathematical modelling

The BET model was correctly adjusted up to an a_w of 0.57, while the GAB model was adjusted in the entire evaluated range; likewise, the GAB model presented a higher r^2 . Similar results were observed in sweet potato flour (*Ipomoea batata* L.) [34]. The parameters are reported in Table 5.

Table 5. Parameters obtained in the water sorption isotherms mathematical modelling.

Samples	Models		Samples	Models		Samples	Models				
	BET	GAB		BET	GAB		BET	GAB			
Sweet potato	Model constants	$X_0: 0.04$ $C: 17.875$	$X_0: 0.05$ $C: 17.79$ $K: 0.9$	Oca white variety	Model constants	$X_0: 0.05$ $C: 12.5$	$X_0: 0.059$ $C: 13.82$ $K: 0.9$	Oca yellow variety	Model constants	$X_0: 0.051$ $C: 4.443$	$X_0: 0.053$ $C: 4.795$ $K: 0.97$
	Adj. r^2	0.98	0.999		Adj. r^2	0.98	0.98		Adj. r^2	0.98	0.97
	RMSE	0.016	0.022		RMSE	0.0032	0.0037		RMSE	0.02	0.023
	MRPD	19.98	19.99		MRPD	7.052	7.154		MRPD	12.72	13.74
Mashua	Model constants	$X_0: 0.065$ $C: 16.4$	$X_0: 0.07$ $C: 11.47$ $K: 0.96$	Zanahoria blanca	Model constants	$X_0: 0.051$ $C: 15.24$	$X_0: 0.055$ $C: 12.13$ $K: 0.91$	Oca red variety	Model constants	$X_0: 0.055$ $C: 21.89$	$X_0: 0.057$ $C: 20.26$ $K: 0.98$
	Adj. r^2	0.989	0.999		Adj. r^2	0.972	0.988		Adj. r^2	0.989	0.998
	RMSE	0.004	0.005		RMSE	0.01	0.013		RMSE	0.01	0.011
	MRPD	19.999	19.999		MRPD	19.07	19.87		MRPD	12.56	13.74

The moisture of the monolayer (X_0) determines the bound moisture of the food [35]. The constant C is known as the sorption heat and relates the active sites of the food matrix and the water molecules of the atmosphere. The shape curve is related to the C value; when its value is greater than 2, it means there is an inflection point in the curve. Therefore, the isotherm is type II, and the food shows an adsorption capacity of water in multilayers. The correction factor of the multilayer sorption constant (K) of the GAB model should be <1 , and it represents the interaction of water molecules in the multilayer [36].

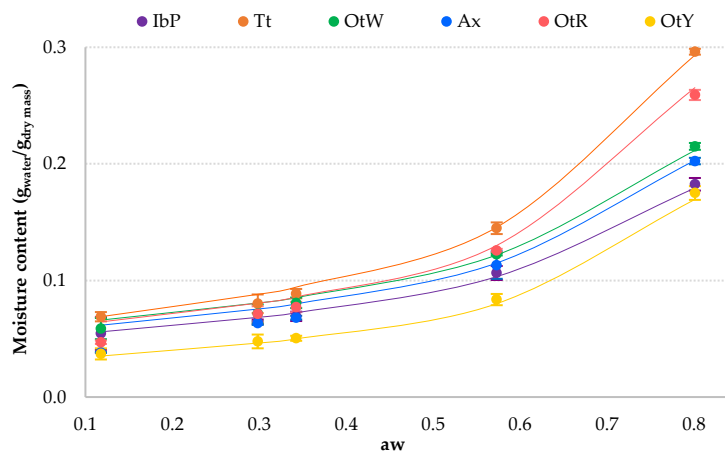


Figure 2. Experimental water sorption isotherms at 20°C and estimated curves using the GAB model (IbP: purple sweet potato, Tt: mashua, Ax: zanahoria blanca, OtW: Oca white variety, OtY: Oca yellow variety, OtR: Oca red variety).

4. Conclusions

The drying process at 65°C for 8 hours showed three precise stages. The first stage of adaptation was where the humidity of the food was reduced minimally—subsequently, the drying period was at a constant velocity, presenting an approximately linear trend. The third stage showed a gradual drop in the drying rate. The experimental data were satisfactorily adjusted to 7 mathematical models, highlighting the Page model (higher r^2). The isotherms showed a type II sigmoidal shape, representing the samples are hygroscopic due to the structural changes suffered by the process. All the matrices must be dried until reaching a humidity below 10 $g_{water}/g_{dry\ mass}$ and stored in environments with an HR lower than 60% to remain stable. Finally, the GAB showed a higher r^2 .

Author Contributions: Conceptualization, L.A. and M.I.; data curation, L.A., A.B., A.Bo, and M.V.; writing—original draft preparation, L.A.; writing—review and editing, P.G.-S., J.M.-M., and M.I. All authors have read and agreed to the published version of the manuscript.

Data Availability Statement: Data is contained within the article.

Acknowledgments: The authors are grateful to the Centro de Cooperación al Desarrollo (CCD) of the Universitat Politècnica de València (project AD2111) and the Dirección de Investigación y Desarrollo (DIDE) of the Technical University of Ambato (Resolution UTA-CONIN-2022-0269-R), for financing the project “Valorización de tubérculos andinos para la obtención de ingredientes alimentarios y su viabilidad. Concienciación de su valor nutritivo y funcional”.

Conflicts of Interest: The authors declare no conflict of interest.

References

- Flores, H.E.; Walker, T.S.; Guimaraes, R.L.; Bais, H.P.; Vivanco, J.M. Andean root and tuber crops: Underground rainbows. *HortScience* **2003**, *38*, 161-168.
- Alam, M.K. A comprehensive review of sweet potato (*Ipomoea batatas* [L.] Lam): Revisiting the associated health benefits. *Trends in Food Science & Technology* **2021**, *115*, 512-529, doi:<https://doi.org/10.1016/j.tifs.2021.07.001>.
- Guevara-Freire, D.A.; Valle-Velástegui, L.; Barros-Rodríguez, M.; Vásquez, C.; Zurita-Vásquez, H.; Dobronski-Arcos, J.; Pomboza-Tamaquiza, P. Nutritional composition and bioactive components of mashua (*Tropaeolum tuberosum* Ruiz and Pavón). *Tropical Subtropical Agroecosystems* **2018**, *21*.
- Ayala, G. Aporte de los cultivos andinos a la nutrición humana. In *Raíces Andinas: Contribuciones al conocimiento y a la capacitación. I. Aspectos generales y recursos genéticos de las raíces andinas*, Seminario, J., Ed.; International Potato Center: Lima, Perú, 2004; pp. 101-112.
- Zhu, F.; Cui, R. Comparison of physicochemical properties of oca (*Oxalis tuberosa*), potato, and maize starches. *International Journal of Biological Macromolecules* **2020**, *148*, 601-607, doi:<https://doi.org/10.1016/j.ijbiomac.2020.01.028>.
- Jimenez, M.E.; Rossi, A.; Sammán, N. Health properties of oca (*Oxalis tuberosa*) and yacon (*Smallanthus sonchifolius*). *Food function* **2015**, *6*, 3266-3274.
- Aniesrani Delfiya, D.; Prashob, K.; Murali, S.; Alfiya, P.; Samuel, M.P.; Pandiselvam, R. Drying kinetics of food materials in infrared radiation drying: A review. *Journal of Food Process Engineering* **2022**, *45*, doi:doi.org/10.1111/jfpe.13810.
- Troller, J. *Water activity and food*; Elsevier: 2012.
- Wang, J.; Yang, X.-H.; Mujumdar, A.; Wang, D.; Zhao, J.-H.; Fang, X.-M.; Zhang, Q.; Xie, L.; Gao, Z.-J.; Xiao, H.-W. Effects of various blanching methods on weight loss, enzymes inactivation, phytochemical contents, antioxidant capacity, ultrastructure and drying kinetics of red bell pepper (*Capsicum annuum* L.). *LWT* **2017**, *77*, 337-347.
- Shazman, A.; Mizrahi, S.; Cogan, U.; Shimoni, E. Examining for possible non-thermal effects during heating in a microwave oven. *Food Chemistry* **2007**, *103*, 444-453.
- Farhat, A.; Fabiano-Tixier, A.-S.; El Maataoui, M.; Maingonnat, J.-F.; Romdhane, M.; Chemat, F. Microwave steam diffusion for extraction of essential oil from orange peel: Kinetic data, extract's global yield and mechanism. *Food chemistry* **2011**, *125*, 255-261.
- Shen, H.; Fan, D.; Huang, L.; Gao, Y.; Lian, H.; Zhao, J.; Zhang, H. Effects of microwaves on molecular arrangements in potato starch. *RSC advances* **2017**, *7*, 14348-14353.
- Lewandowicz, G.; Fornal, J.; Walkowski, A. Effect of microwave radiation on physico-chemical properties and structure of potato and tapioca starches. *Carbohydrate Polymers* **1997**, *34*, 213-220.
- Acurio, L.; Salazar, D.; García-Segovia, P.; Martínez-Monzó, J.; Igual, M. Third-Generation Snacks Manufactured from Andean Tubers and Tuberous Root Flours: Microwave Expansion Kinetics and Characterization. *Foods* **2023**, *12*, 2168.
- Salazar, D.; Arancibia, M.; Ocaña, I.; Rodríguez-Maecker, R.; Bedón, M.; López-Caballero, M.E.; Montero, M.P. Characterization and technological potential of underutilized ancestral andean crop flours from Ecuador. *Agronomy* **2021**, *11*, 1693.
- O'Callaghan, J.R.; Menzies, D.J.; Bailey, P.H. Digital simulation of agricultural drier performance. *Journal of Agricultural Engineering Research* **1971**, *16*, 223-244, doi:[https://doi.org/10.1016/S0021-8634\(71\)80016-1](https://doi.org/10.1016/S0021-8634(71)80016-1).
- Page, G.E. Factors Influencing the Maximum Rates of Air Drying Shelled Corn in Thin layers. Purdue University, 1949.
- Overhults, D.G.; White, G.; Hamilton, H.; Ross, I. Drying soybeans with heated air. *Transactions of the ASAE* **1973**, *16*, 112.
- Henderson, S.M.; Pabis, S. Grain drying theory, I. Temperature effect on drying coefficient. *Journal of Agricultural Engineering Research* **1961**, *6*, 169-173.
- Yagcioglu, A. Drying characteristic of laurel leaves under different conditions. In Proceedings of the Proceedings of the 7th International congress on agricultural mechanization and energy, 1999; pp. 565-569.
- Thompson, T.L.; Peart, M.; Foster, G.H. Mathematical Simulation of Corn Drying — A New Model. *Transactions of the ASAE* **1968**, *11*, 582-586, doi:<https://doi.org/10.13031/2013.39473>.
- Crank, J. *The mathematics of diffusion*; Oxford university press: 1979.
- Greenspan, L. Humidity fixed points of binary saturated aqueous solutions. *Journal of research of the National Bureau of Standards* **1977**, *81*, 89.

24. Spiess, W.E.; Wolf, W. Critical evaluation of methods to determine moisture sorption isotherms. In *Water activity: theory and applications to food*; Routledge: 2017; pp. 215-233. 1
25. Honorable Provincial Government of Tungurahua. Tungurahua Hydrometeorological Network. Available online: https://rrnn.tungurahua.gob.ec/red/promedios_mensuales (accessed on 2023, 10, 14). 2
26. Brunauer, S.; Emmett, P.H.; Teller, E. Adsorption of gases in multimolecular layers. *Journal of the American chemical society* **1938**, *60*, 309-319. 3
27. Van den Berg, C.; Bruin, S. Water activity and its estimation in food systems. In Proceedings of the Proceedings Int. Symp. Properties of Water in Relation to Food Quality and Stability, Osaka, 1978, 1978. 4
28. Restrepo Victoria, Á.H.; Burbano Jaramillo, J.C. Disponibilidad térmica solar y su aplicación en el secado de granos. *Scientia et technica* **2005**, *1*, 127-132. 5
29. Ananias, R.A.; Vallejos, S.; Salinas, C. Estudio de la cinética del secado convencional y bajo vacío del pino radiata. *Maderas. Ciencia y tecnología* **2005**, *7*, 37-47. 6
30. García-Mogollón, C.; Torregroza-Espinosa, A.; Sierra-Bautista, M. Cinética de Secado de Chips de Yuca (*Manihot esculenta crantz*) en Horno Microondas. *Revista Técnica de la Facultad de Ingeniería Universidad del Zulia* **2016**, *39*, 098-103. 7
31. Salcedo-Mendoza, J.; Contreras-Lozano, K.; García-López, A.; Fernandez-Quintero, A. Modelado de la cinética de secado del afrecho de yuca (*Manihot esculenta Crantz*). *Revista Mexicana de Ingeniería Química* **2016**, *15*, 883-891. 8
32. Navia, D.; Ayala, A.; Villada, H.S. Isotermas de adsorción de bioplásticos de harina de yuca moldeados por compresión. *Biotecnología en el Sector Agropecuario y Agroindustrial* **2011**, *9*, 77-87. 9
33. Martins Oyinloye, T.; Byong Yoon, W. Effect of freeze-drying on quality and grinding process of food produce: A review. *Processes* **2020**, *8*, 354. 10
34. Saavedra Layza, G.E. Efecto de la temperatura en el valor de monocapa de harina de camote (*Ipomoea batata L.*) variedad amarilla mediante la isoterma de GAB. *TAGI* **2022**. 11
35. Gutierrez Balarezo, J.; Diaz Viteri, J.E.; Mendieta Taboada, O.W.; Pulla Huilca, P.V.; Chañi Paucar, L.O. Conservación de la harina de plátano (*Musa paradisiaca*) en Puerto Maldonado, Madre de Dios. *Biodiversidad Amazónica* **2019**, *4*. 12
36. Ceballos, A.M.; Giraldo, G.I.; Orrego, C.E. Evaluacion de varios modelos de isotermas de adsorción de agua de un polvo de fruta deshidratada. *Vector* **2009**, 107-117. 13